Taylor & Francis
Taylor & Francis Group

Radiation Effects and Defects in Solids
Incorporating Plasma Science and Plasma Technology

ISSN: (Print) (Online) Journal homepage: https://www.tandfonline.com/loi/grad20

Properties of cement Portland composite prepared with Barium sulfate and Bismuth oxide for radiation shielding

Gunjanaporn Tochaikul, Manus Mongkolsuk, Phetnarin Kobutree, Supannika Kawvised, Phornpailin Pairodsantikul, Paramest Wongsa & Nutthapong Moonkum

To cite this article: Gunjanaporn Tochaikul, Manus Mongkolsuk, Phetnarin Kobutree, Supannika Kawvised, Phornpailin Pairodsantikul, Paramest Wongsa & Nutthapong Moonkum (28 Dec 2023): Properties of cement Portland composite prepared with Barium sulfate and Bismuth oxide for radiation shielding, Radiation Effects and Defects in Solids, DOI: 10.1080/10420150.2023.2294037

To link to this article: https://doi.org/10.1080/10420150.2023.2294037

Published online: 28 Dec 2023.

RADIATION EFFECTS & DEFECTS IN SOLIDS
https://doi.org/10.1080/10420150.2023.2294037

Taylor & Francis
Taylor & Francis Group

Check for updates

Properties of cement Portland composite prepared with Barium sulfate and Bismuth oxide for radiation shielding

Gunjanaporn Tochaikul [a], Manus Mongkolsuk[a], Phetnarin Kobutree[b], Supannika Kawvised[c], Phornpailin Pairodsantikul[c], Paramest Wongsa[c] and Nutthapong Moonkum [a]

[a]Faculty of Radiological Technology, Rangsit University, Patumthani, Thailand; [b]Anatomy Unit, Faculty of science, Rangsit University, Meung Pathumthani, Thailand; [c]School of Radiological Technology, Faculty of Health Science Technology, HRH Princess Chulabhorn College of Medical Sciences, Chulabhorn Royal Academy, Bangkok, Thailand

ABSTRACT

Radiation is useful but can be harmful to humans if used carelessly. Therefore, radiation protection equipment is necessary for workers. In this paper, we aim to study a cement composite with $BaSO_4/Bi_2O_3$ for protection against X-rays and gamma rays. The shielding ability was measured using a diagnostic X-ray with energies of 60–120 keV and gamma rays of Cs-137, Ba-133, Co-57 and the morphology structure was determined including radiation protection properties. The results showed that Portland cement with a high concentration of $BaSO_4/Bi_2O_3$ had the ability to absorb radiation from X-rays in the range of 95.54–99.87% and gamma energy in the range of 93.37–98.88%. Moreover, the composite of $BaSO_4/Bi_2O_3$ induced a homogenous structure of Portland cement possibly affecting the strength of the material. In addition, Portland shielding can be designed for use in related applications in various energy ranges including ones that are environmentally friendly and suitable for the development of radiation protection in the future.

ARTICLE HISTORY
Received 23 September 2023
Accepted 6 December 2023

KEYWORDS
Barium sulfate; bismuth oxide; radiation shielding; X-ray; gamma; Portland cement

1. Introduction

Currently, radiology has extensive studies and research on radiation shielding materials (*1*). The main purpose is to use composites to replace lead shielding in certain applications, particularly when there is a need to reduce the weight (*2*) and toxicity associated with lead (*3*). Because lead has health and environmental concerns associated with its use, it has led to the exploration of alternative materials like composites (*4*).

The alternative usage of composite materials for radiation shielding depends on the specific requirements of the application including the type and energy of radiation being shielded (*5*), weight constraints (*6*) and cost considerations (*7*). For effective radiation shielding, materials with high atomic numbers are preferred because they are more effective at attenuating ionizing radiation (*8*). High atomic numbers have a greater number of protons in their atomic nuclei, which results in stronger interactions with ionizing radiation (*9*). Due

CONTACT Nutthapong Moonkum Nutthapong.m@rsu.ac.th

to a phenomenon known as the photoelectric effect, materials with high atomic numbers demonstrate increased effectiveness in shielding high-energy photons. The photoelectric effect is a process wherein photons interact with matter, transferring their energy to electrons within the material and causing the ejection of these electrons. This phenomenon holds particular significance when dealing with high-energy photons, including X-rays and gamma rays (10). The most commonly used high-Z materials for radiation shielding include Tungsten (W) (11) Bismuth (Bi) (12) Uranium (U) (13) Thorium (Th) (14) and Barium (Ba) (15)

In previous research articles, various materials have been studied for radiation protection, such as epoxy composites with tungsten for Co-60 radiation shielding (16), with $BaSO_4$ (17), Bi_2O_3 (18) or even iodine contrast media (19) for radiation shielding in diagnostic and nuclear medicine. The results showed that adding high atomic number substances to the mixture can greatly reduce the radiation dose.

Furthermore, previous studies investigate the X-ray radiation shielding properties of cement mortars prepared with different types of aggregates such as sand, fine stone, beverage glass, untreated funnel glass, treated funnel glass and barite. Several previously published studies have explored the role of composites in mortar for shielding. The results demonstrated the feasibility of using different types of aggregates in cement mortar for diagnostic X-ray shielding, with the potential for enhancing radiation shielding ability through increased mortar density (20). The investigation by Yao Y, et al. of the shielding ability of a Bi_2O_3-loaded concrete mixture against gamma rays from a 137Cs (662 keV) radioactive source was compared with theoretical values calculated using the XCOM program (21). Kavaz E et al. studies of gamma ray shielding effectiveness of the Portland cement pastes doped with brass-copper found significant gamma absorption (22). Composites cement/$BaSO_4$/Fe_3O_4/CuO was studied by Gharissah M. S, et al. for improving the X-ray absorption characteristics and were successful for the X-ray radiation shield with energies of 55, 66 and 77 keV. These results indicated a high potential for composite designs instead of concrete for new and efficient radiology rooms (23). The study of shielding Mortars for Radiation Source Transportation and storage was prepared and the impact of WO_3 and barite on their radiation shielding performance was evaluated using radioactive sources (Am-241, Cs-137, Eu-152, Ba-133). This material is promising as an effective shield of radiation-emitting sources during transportation and long-term storage (24). Further, preparations of Mortar with Fe_2O_3 Nanoparticles for Cs-137, Co-60 and Am-241 radiation shielding were compared with the XCOM program, and a very good agreement between the theoretical and experimental results was obtained (25). Likewise, Portland cement is the most common type of cement used in construction and has several benefits that make it an ideal choice for a wide range of applications: it has great resistance to cracking and shrinkage but less resistance to chemical attacks (26).

Additionally, $BaSO_4$ is commonly used as a radiopaque contrast agent in medical imaging procedures (27). Barium has a relatively high atomic number ($Z = 56$) (28), which makes it effective at interacting with and absorbing ionizing radiation. This property makes barium sulfate a suitable material for shielding against X-rays and gamma rays (29). Bi_2O_3 is sometimes used in radiation shielding applications, primarily for its high atomic number (Z) and density (30). Bismuth (Bi) has a high atomic number ($Z = 83$) (31), which means it has a greater number of protons in its atomic nucleus. This high atomic number makes bismuth an effective material for attenuating ionizing radiation, particularly gamma rays and X-rays (32). Moreover, $BaSO_4$ and Bi_2O_3 can be considered relatively environmentally friendly when used in controlled and regulated applications. In addition, Portland cement is one of the most widely used construction materials in the world (33). It is a versatile and essential component in various construction applications due to its strength (34), durability (35) and ability to bond with other materials (36).

However, previous studies focused on a single substance and only studied the energy range in diagnostic radiation or nuclear medicine. For that reason, this study aims to investigate the Portland radiation shielding properties with composites of $BaSO_4$ and Bi_2O_3 for both radiation protection in X-ray and gamma rays. The knowledge from this research may help create radiation-shielding materials in each area. In addition, the resulting material is environmentally friendly.

2. Material and methods

2.1. Raw materials

Commercial Portland cement (ASTM C-150) was obtained from the local company (TPI Polene Public Company Limited, Thailand). The chemical composition of cement determined by X-ray fluorescence spectrometer (XRF) is presented in Table 1. Barium sulfate ($BaSO_4$) with purity of 99% was provided by KEMAUS (Australia) and powder bismuth oxide (Bi_2O_3) with purity of 99.9% was provided by Thermo Fisher Scientific (Belgium). The physical appearances of the raw materials are shown in Figure 1.

2.2. Preparation of Portland radiation shielding

The materials were mixed for 10 min in a mixing machine with 4 formulations (%w/w) as shown in Table 2 and then, the material was added to the block (10 × 10 × 2 cm) for X-ray shielding and thickness 5 cm for gamma shielding. After that, the materials were cured at

Table 1. The chemical composition of base materials used in the research work.

Constituent	CaO	SiO_2	Al_2O_3	MgO	Fe_2O_3	SO_3	K_2O	Na_2O
Percentage	50.60	15.20	2.28	1.54	1.22	1.16	0.19	0.127

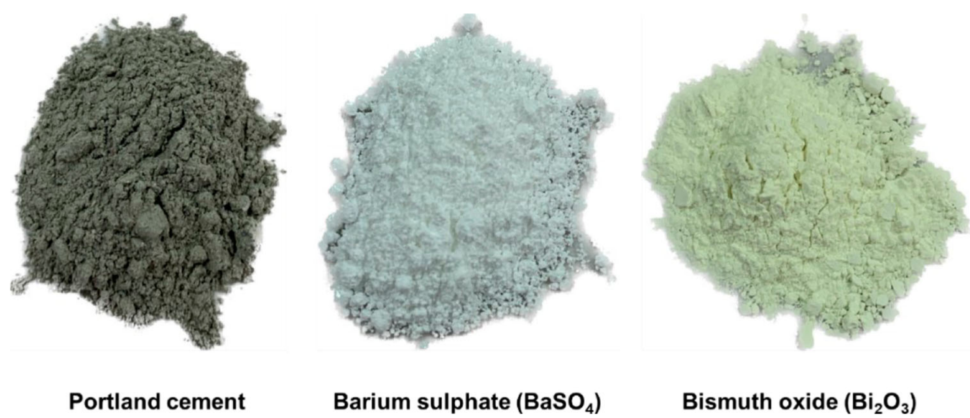

Figure 1. Raw materials.

Table 2. Mixture percentage of prepared Portland cement.

Sample	Composition			
	Portland cement (%)	$BaSO_4$ (%)	Bi_2O_3 (%)	Water (%)
Sample 1: Control	100	–	–	50
Sample 2: 10% $BaSO_4 + Bi_2O_3$	90	5	5	50
Sample 3: 20% $BaSO_4 + Bi_2O_3$	80	10	10	50
Sample 4: 30% $BaSO_4 + Bi_2O_3$	70	15	15	50

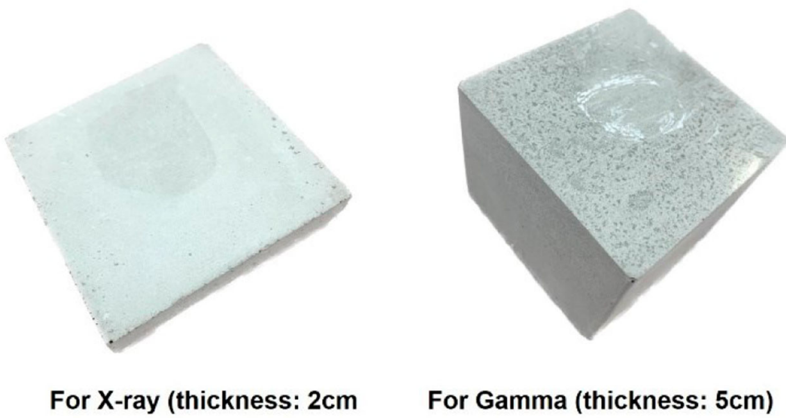

Figure 2. The Portland cement sample in the radiation shielding properties.

room temperature for 30 days and removed from the molds prior to testing. The samples are shown in Figure 2.

2.3. Characterization of Portland radiation shielding

The scanning electron microscope (SEM) images: The sample of material shielding was broken and then mounted on a stub. The assemblies were dried under reduced pressure at an ambient temperature overnight, and then coated with a thin layer of gold prior to observation. The morphology of material shielding was observed by JEOL JSM-IT300 scanning electron microscope (USA) with an operating voltage of 15 kV. SEM-EDS was applied to check the chemical composition of $BaSO_4$ and Bi_2O_3 in Portland cement shielding material.

Tensile testing of Portland radiation shielding: For strength measurement, a tensile strength test (1TK-10TX, BEMAX, Osaka, Japan) loading at 1–10 ton and X-ray fluorescence spectrometer–XRF (BRUKER S8 TIGER) analyzed the chemical composition of base materials of Portland cement.

2.4. X-ray and gamma-ray shielding experiment

The radiation absorption properties were measured from the X-ray with the applied energy voltages ranging from 60–120 kVp irradiated by general X-ray (FDR smart X/Fujifilm) and gamma ray were measured from a standard source of Cs-137 (662 keV), Ba-133 (31, 356, 81 and 303 keV), Co-57 (122 keV). The cement material shielding was irradiated by X-ray (FDR

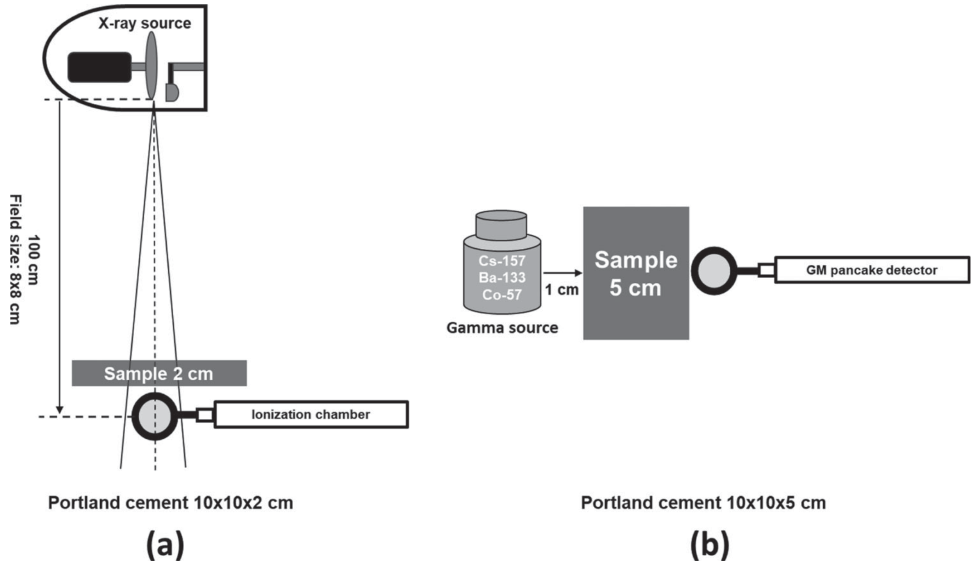

Figure 3. Schematic of experimental setup of radiation shielding test (a) X-ray test (b) Gamma test.

smart X/Fujifilm) at a distance of 100 cm from the X-ray source and a field size of 8 × 8 cm. The X-ray dose was measured by Radcal Accu Gold and gamma ray was irradiated at a distance of 1 cm from standard source. The gamma ray dose was measured by GM pancake detector (Ludlum offers our Model 44-9 GM pancake detector) as seen in Figure 3.

The properties of radiation shielding such as radiation absorption, linear attenuation coefficient, HVL and TVL were described by the following Equations (1)–(3)

$$\text{Linear attenuation coefficient} = I = I_0 \cdot e^{-\mu x} \tag{1}$$

$$\text{HVL} = \frac{0.693}{\mu} \tag{2}$$

$$\text{TVL} = \frac{2.303}{\mu} \tag{3}$$

I: The intensity of the radiation after passing through the material.
I_0: The initial or incident intensity of the radiation before passing through the material.
μ: The attenuation coefficient. X: The thickness or path length of the material.

3. Results

3.1. Characterization and morphology of Portland cement radiation shielding

The density values of the Portland cement samples were 1.44, 1.966, 2.492 and 3.018 g/cm^3 for Portland (without $BaSO_4$ and Bi_2O_3), with 10%, 20% and 30% $BaSO_4$ respectively. In general, $BaSO_4$ and Bi_2O_3 have higher molecular weight and density (37, 38), as compared to pure bismuth (Bi) due to the arrangement of atoms in a crystal lattice (39). The result of this experiment found that composites of $BaSO_4$ and Bi_2O_3 had increased density in Portland cement (Figure 4).

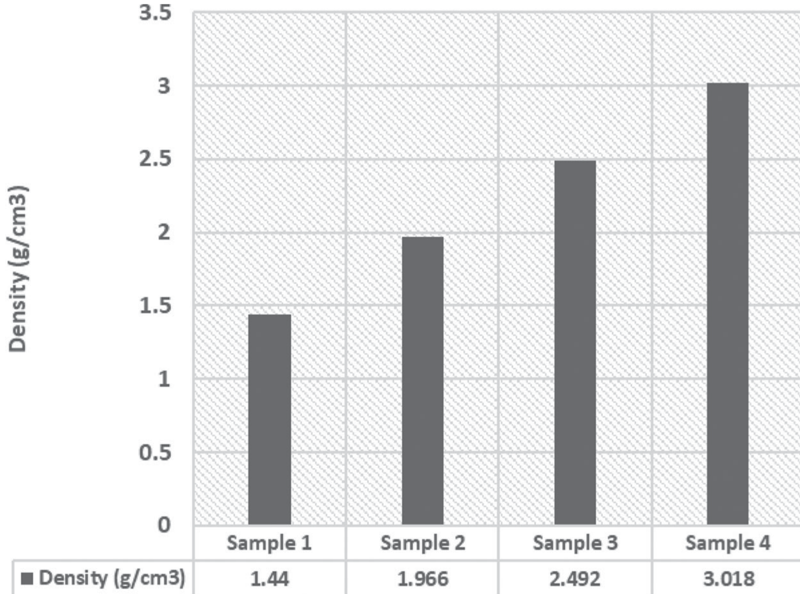

Figure 4. Density of the Portland cement samples.

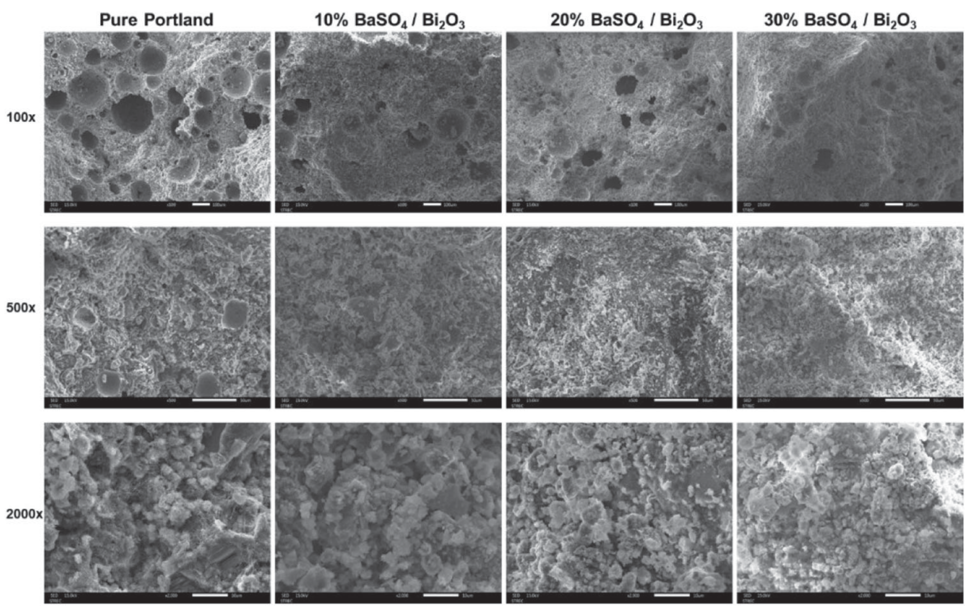

Figure 5. The SEM image with morphology of Portland cement at 100×, 500× and 2000×.

A scanning electron microscope (SEM) of the JSM-IT300, JEOL model was used to produce morphological images of the prepared Portland cement samples, as shown in Figure 5. The figure shows that the distribution of $BaSO_4$ and Bi_2O_3 is more homogeneous with increased percentages of $BaSO_4$ and Bi_2O_3.

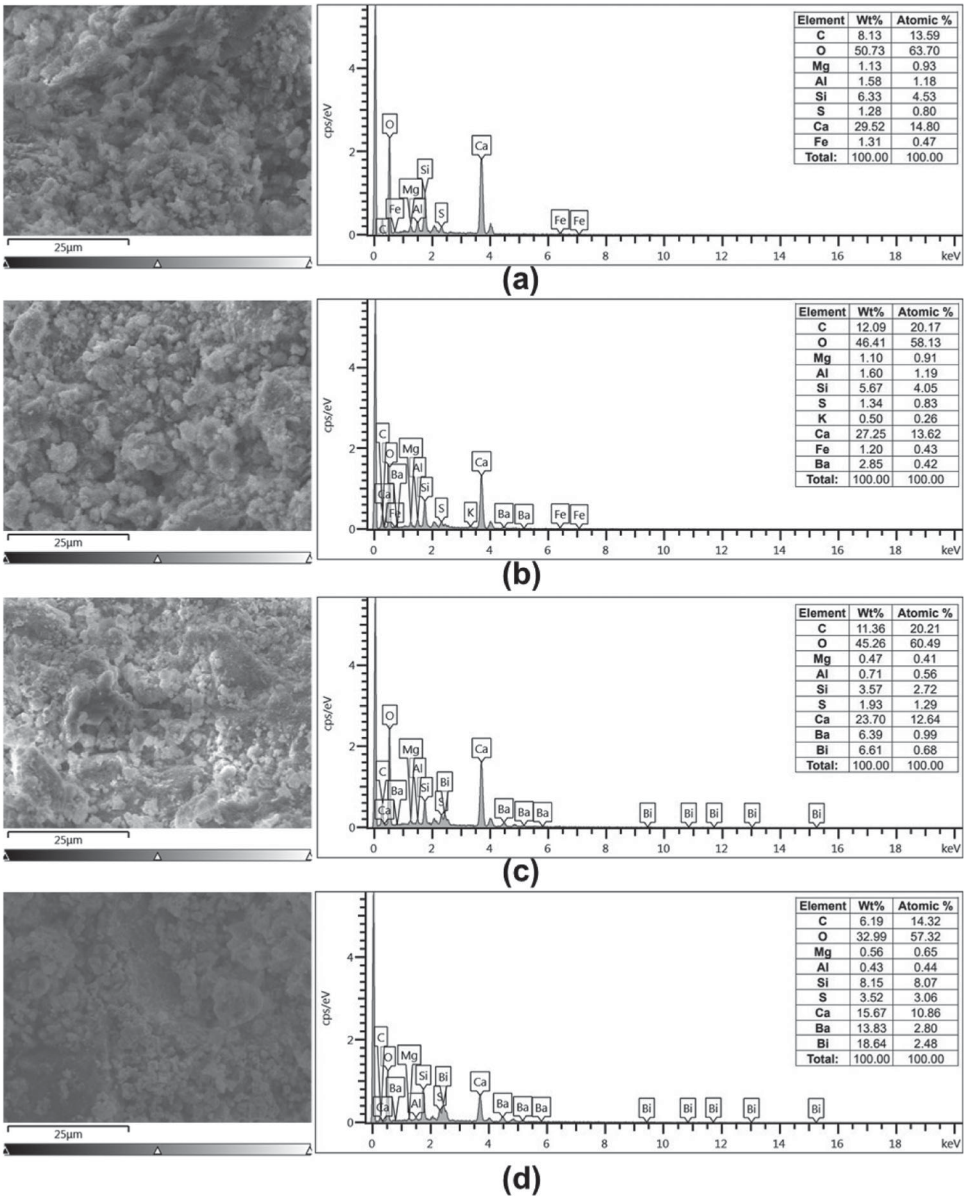

Figure 6. Result of SEM-EDS analysis. EDS spectrum of Portland cement (a) sample 1 or control (b) sample 2 (c) sample 3 and (d) sample 4.

The SEM-EDS for chemical analysis in Portland cement material are shown in Figure 6. Figure 6(b–d) reveals that the composite of Ba and Bi increases with increasing concentration of $BaSO_4$ and Bi_2O_3. But in sample 2, (formula of 10% $BaSO_4$ and Bi_2O_3) Bi was not detected in the composite which may have been caused by mixing in the forming process.

However, the morphology from SEM can be confirmed as composite $BaSO_4$ and Bi_2O_3 were mixed in Portland cement and it also results in the material being more homogenous when increasing the composite of $BaSO_4$ and Bi_2O_3.

3.2. Compressive strength

The compressive strength of the Portland cement decreased as the combined loading of $BaSO_4$ and Bi_2O_3. Figure 7 shows that the force, tensile strength and tensile stress are decreased when increasing the concentration of $BaSO_4$ and Bi_2O_3. Figure 7(a) shows the maximum force (kN) of Portland cement with composite of $BaSO_4$ and Bi_2O_3 as 99.47, 99.12, 98.96 and 98.59 kN, respectively. Figure 7(b) indicates the maximum strength (N/mm) of Portland cement with composite of $BaSO_4$ and Bi_2O_3 as 994.72, 991.29, 989.62 and 985.95 N/mm, respectively and in Figure 7(c) the maximum stress of Portland cement with composite of $BaSO_4$ and Bi_2O_3 as 58.51, 58.31, 58.21 and 57.997, respectively. The results show that the composite of $BaSO_4$ and Bi_2O_3 can affect Portland cement strength by reducing compressive strength when increasing the concentration of $BaSO_4$ and Bi_2O_3.

3.3. X-ray and gamma-ray shielding properties

The radiation of X-ray shielding properties was determined from the exposure technique 60–120 kVp and gamma ray using standard source from radioactive in the energy range of 31–662 keV (Co57, Ba133 Cs137). Portland cement with a concentration of 15% $BaSO_4$ and 15% Bi_2O_3 at thickness of 2 cm for X-ray test and 5 cm for gamma test had higher shielding efficiencies for reducing the radiation dose from X-ray and gamma ray as depicted in Figure 8(a) and 8(b). Additionally, the radiation shielding abilities of the Portland cement with lead were compared in both X-ray and gamma ray and found that the radiation shielding properties in high concentration of $BaSO_4$ and Bi_2O_3 are similar in X-ray test but are less than lead in gamma test. For Figure 9(a), the radiation after shielding by lead did not detect radiation from Co-57 and very low in Ba-133 as 0.22 mSv/hr and not shown in the histogram. As a result, the linear attenuation, HVL and TVL values cannot be determined.

In addition, Portland cement with composite of $BaSO_4$ and Bi_2O_3 was good at reducing radiation at low energy and blocking ability decreased with the increasing irradiation energy and found that the shielding properties increased with an increasing composite of $BaSO_4$ and Bi_2O_3.

3.4. Radiation absorption properties, linear attenuation coefficient, HVL and TVL

The other shielding parameter properties based on our research work such as radiation absorption, linear attenuation coefficient, HVL and TVL were calculated by the following Equations: (1)–(3). The results demonstrate that the radiation absorption increased with an increased composite of $BaSO_4$ and Bi_2O_3. Higher concentrations in Portland cement (15% $BaSO_4$ and 15% Bi_2O_3) show all absorption characteristics from the experimental data in this study are higher in both X-ray in 60, 80, 100 and 120 kVp was 99.87, 98.98, 97.09 and 95.54%, respectively in Figure 9(a) and gamma energy in the energy range of 31–662 keV (Co-57, Ba-133 Cs-137) was 98.88, 96.79 and 93.37%, respectively in Figure 9(b).

The linear attenuation properties of radiation shielding material increased when composite of $BaSO_4$ and Bi_2O_3 was increased. Portland cement with 30% $BaSO_4/Bi_2O_3$ demonstrated higher shielding efficiencies as shown in Figure 10.

Additionally, the half-value layer (HVL) and tenth-value layer (TVL) were investigated to evaluate the performance of the X-ray shielding. For all Portland cement samples, the HVL

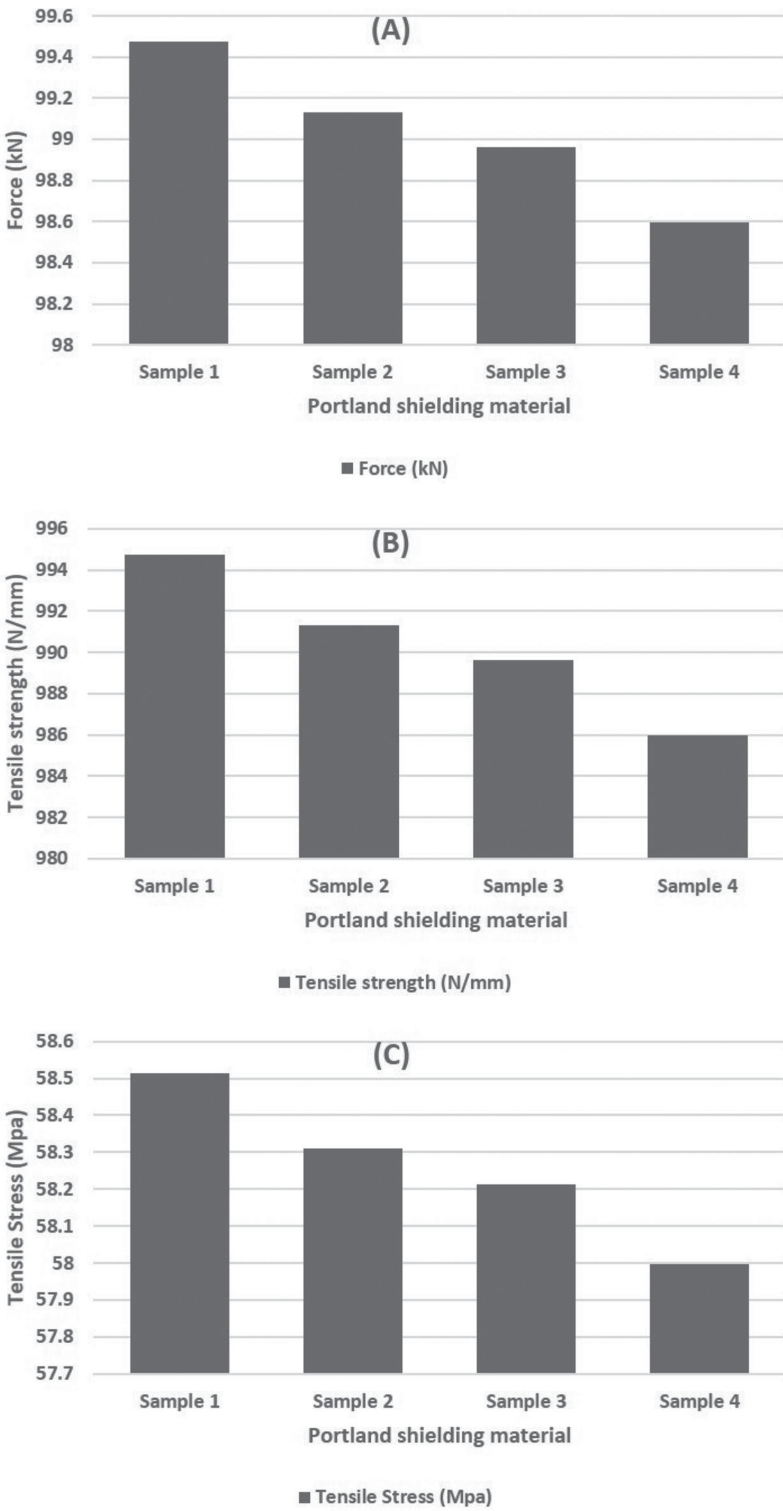

Figure 7. The compressive strength. (a) Force (b) Tensile strength and (c) Tensile stress.

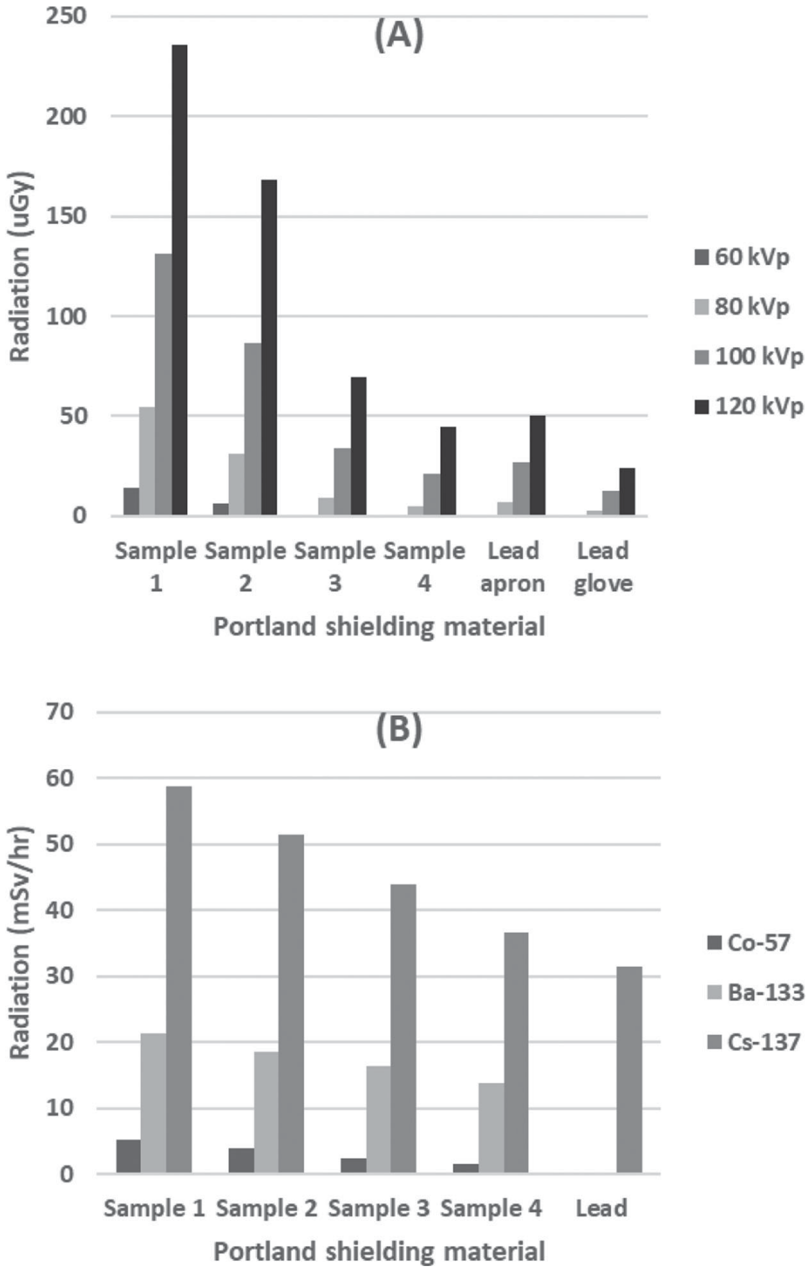

Figure 8. (a) The radiation dose (X-ray) measurement from 60, 80, 100 and 120 kVp and (b) The radiation dose (gamma) measurement from energy 31–662 keV.

and TVL seemed to have increased with an increasing composite of $BaSO_4$ and Bi_2O_3. However, Portland cement composite with 30% $BaSO_4/Bi_2O_3$ compared with 5 mm lead glove, lead apron and 2.5 cm L-lead shielding showed less shield ability. X-ray testing found that the efficiency was similar to lead but less than lead in gamma test in all parameters (Figures 11 and 12).

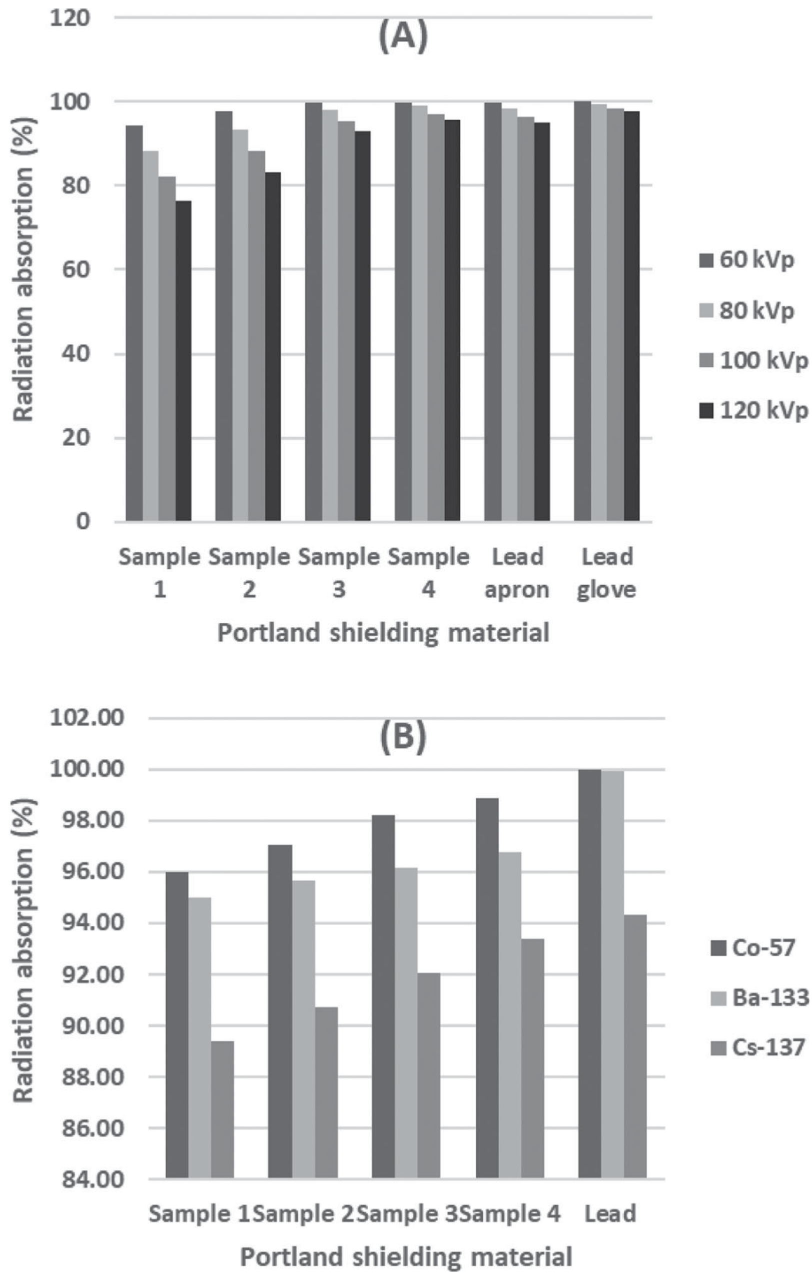

Figure 9. (a) The radiation absorption from 60, 80, 100 and 120 kVp and (b) The radiation absorption measurement from energy 31–662 keV.

4. Discussion and conclusion

Radiation shielding devices are crucial in various radiology departments, industries and applications where ionizing radiation is present (40). The primary purpose of radiation shielding devices is to protect the health and safety of individuals working in environments

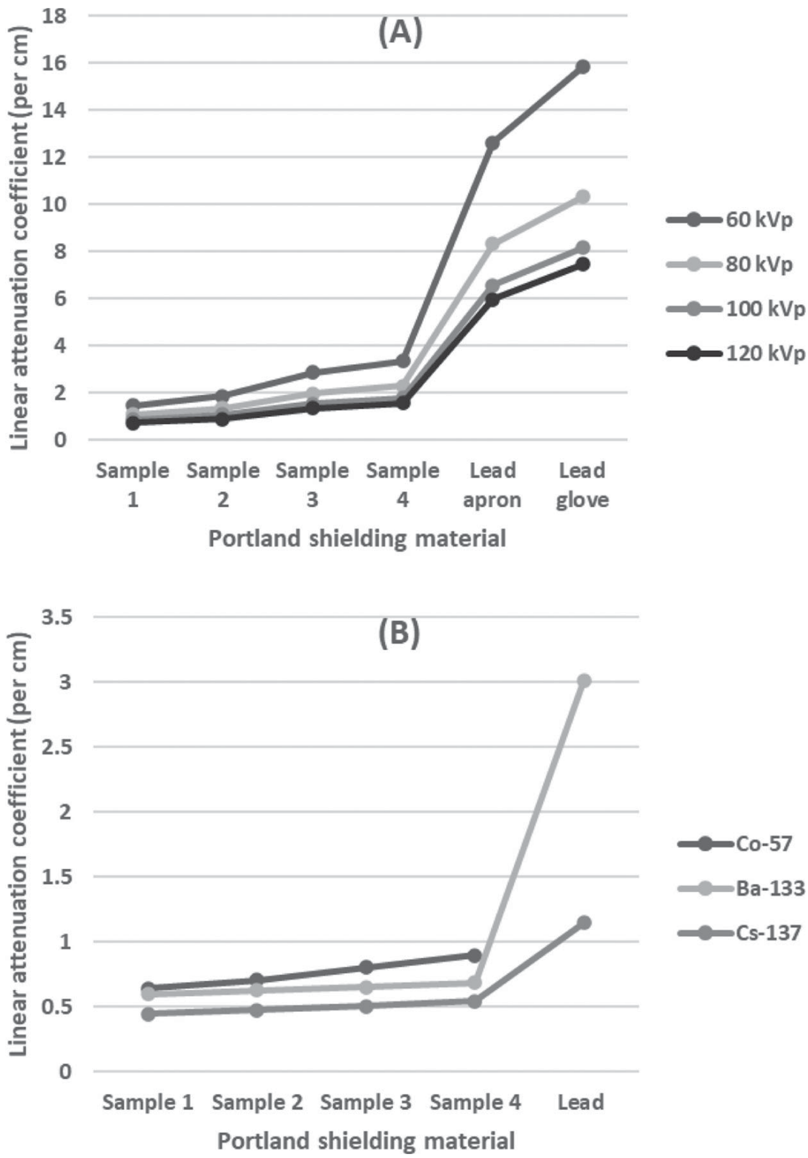

Figure 10. Linear attenuation coefficient of Portland cement (a) X-ray test and (b) Gamma test.

with ionizing radiation (*41*) because radiation can have various detrimental effects on the human cellular components (*42*–*45*) especially, DNA damage which can lead to mutations and cancer (*46*). Therefore, radiation shielding equipment is necessary to prevent radiation hazards.

In this experiment, we compared Portland cement composite with $BaSO_4$ and Bi_2O_3 compared to standard lead shielding. The shielding material from composite of Portland cement with substances of $BaSO_4$ and Bi_2O_3 had good radiation absorption for X-ray but still less than gamma ray. The research is consistent with the previous theory that Gamma rays and X-rays consist of high-energy waves (*47*), especially those with high energy have

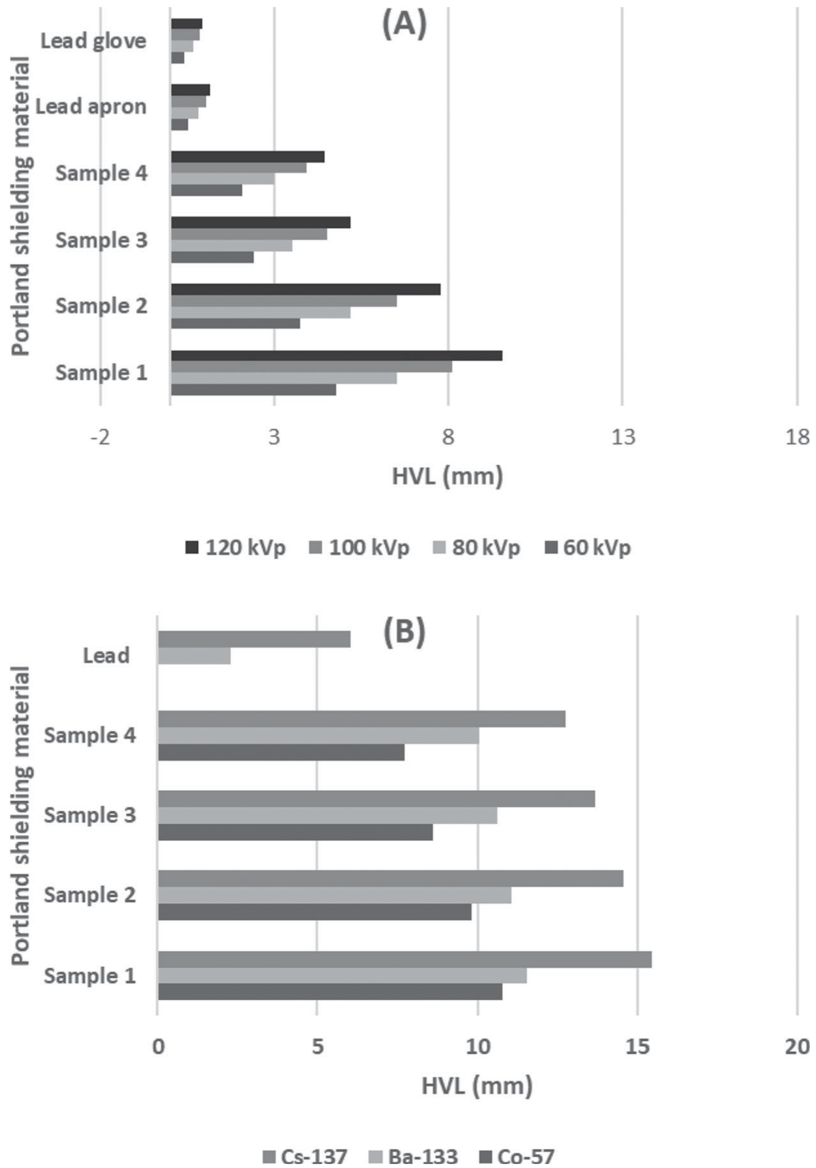

Figure 11. Half-value layer (HVL) (a) X-ray test and (b) Gamma test.

a great ability to penetrate other materials and can penetrate matter easily (*48*). The ability to penetrate matter increases with increasing energy (*48*) and decreases with increasing atomic number of the absorbing material (*49*).

In our research we found that the characteristics of Bi_2O_3 have more density and atomic number than $BaSO_4$ (*50*, *51*), resulting in high efficiency of radiation attenuation in Portland cement. However, the Portland composite with 30% $BaSO_4/Bi_2O_3$ had efficiency of radiation absorption for X-ray (99.87%) similar to lead apron (99.81%) and lead glove (99.96%). In contrast, the efficiency of radiation absorption for gamma rays (93.37%) was less than L-lead shield (97.31%).

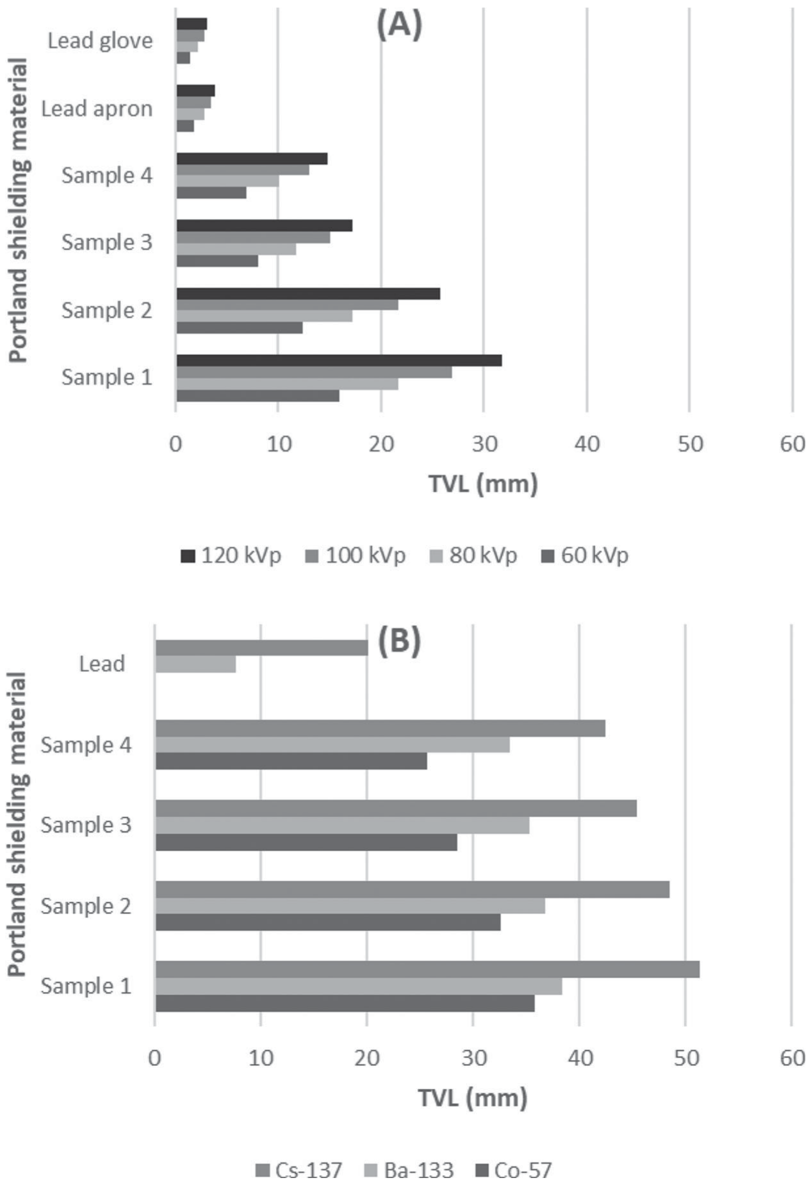

Figure 12. Tenth-value layer (TVL) (a) X-ray test and (b) Gamma test.

In addition, the morphology structure of Portland cement by scanning electron microscopy found that the morphology was homogenous in the Portland cement with $BaSO_4$ and Bi_2O_3 more than pure Portland cement. This effect is likely related to the small particle size and shape of bismuth and barium which are less than the particle size of Portland cement components (52). Typically, the increased solubility of smaller dissolved substances is linked to their favorable interactions with the solvent, larger surface area, and reduced energy needed to break intermolecular forces. Together, these elements play a crucial role in generating highly homogeneous solutions (53). As a result, substances can be mixed together homogeneously. However, this affects the strength of the cement because bismuth and barium have less cohesive and hardening properties than the components in the Portland cement. As a result, the compressive strength is decreased with increasing concentrations of bismuth and barium. The results of this study are related to the integration of bismuth and barium with the components of Portland cement at a chemical level may be problematic, potentially resulting in the formation of less stable compounds. This, in turn, can have adverse effects on the overall strength and cohesion of the cement matrix (*54*); the bismuth and barium composite may exhibit differences in particle size and distribution compared to pure Portland cement. These variations in particle characteristics can influence the packing density of the cementitious material, potentially resulting in a matrix that is less cohesive and weaker (*55*). Moreover, the binding capacity of bismuth and barium might not be equivalent to that of the components in pure Portland cement. The binding capacity plays a crucial role in forming a robust and cohesive cement matrix. If the composite lacks efficient binding, it could lead to a decrease in strength (*56*). Therefore, the mixing and forming process should be improved in order to increase the strength of the material, for example, adding substances that help the material to hold together by strong bonding and strength, including being developed for use in various radiological applications. The type and quantity of aggregates in the concrete are important components for radiation protection properties of concretes (*57, 58*).

The results of the experiments are consistent with research that has mixed $BaSO_4$ and Bi_2O_3 and are known radiation shielding composites in various materials such as polyethylene (*59*), Polyvinyl chloride (*60*), Epoxy Resins (*17*), Silicon rubber (*61*) and gypsum board (*62*). The choice of material will depend on factors such as the type of radiation being shielded (*e.g.* gamma rays, X-rays, neutrons) (*63*), the required thickness of the shielding (*64*), the physical properties needed (flexibility, rigidity or density) (*65*) and cost considerations (*66*).

Ongoing research for radiation shielding (*67, 68*) using Portland cement, which is versatile and durable makes it a fundamental building material in construction and civil engineering (*69*), playing a critical role in the development of infrastructure and buildings worldwide (*70*).

Based on this information, the goal is to create shielding material for diagnostic radiology and nuclear medicine departments using composites of Portland cement with $BaSO_4$ and Bi_2O_3 that compare favorably to traditional lead shielding. This study will be useful for the selection and fabrication of radiation shielding materials that are locally available, inexpensive, easy to mold, nontoxic to manufacture and have similar properties to lead.

Acknowledgements

We would like to express thanks to the School of Radiological Technology, Faculty of Health Science Technology, HRH Princess Chulabhorn College of Medical Sciences, Chulabhorn Royal Academy for radiopharmaceutical testing facilities support and research institute of Rangsit University for research findings.

Disclosure statement

No potential conflict of interest was reported by the author(s).

Funding

This research was supported by the Research Institute of Rangsit University.

Notes on contributors

Gunjanaporn Tochaikul, Lecturer in Faculty of Radiological Technology, Rangsit University, Patumthani, Thailand.

Manus Mongkolsuk, Lecturer in Faculty of Radiological Technology, Rangsit University, Patumthani, Thailand.

Phetnarin Kobutree, Lecturer in Anatomy Unit, Faculty of Science, Rangsit University, Meung Pathumthani, Thailand.

Supannika Kawvised, Lecturer in School of Radiological Technology, Faculty of Health Science Technology, HRH Princess Chulabhorn College of Medical Sciences, Chulabhorn Royal Academy, Bangkok, Thailand.

Phornpailin Pairodsantikul, Lecturer in School of Radiological Technology, Faculty of Health Science Technology, HRH Princess Chulabhorn College of Medical Sciences, Chulabhorn Royal Academy, Bangkok, Thailand.

Paramest Wongsa, Lecturer in School of Radiological Technology, Faculty of Health Science Technology, HRH Princess Chulabhorn College of Medical Sciences, Chulabhorn Royal Academy, Bangkok, Thailand.

Nutthapong Moonkum, Lecturer in Faculty of Radiological Technology, Rangsit University, Patumthani, Thailand.

ORCID

Gunjanaporn Tochaikul http://orcid.org/0000-0003-0049-9676
Nutthapong Moonkum http://orcid.org/0000-0001-7493-3530

References

(1) More, C.V.; Alsayed, Z.; Badawi, M.S.; Thabet, A.A.; Pawar, P.P. Polymeric Composite Materials for Radiation Shielding: A Review. *Environ. Chem. Lett.* **2021,** *19,* 2057–2090.
(2) Vignesh, S.; Winowlin Jappes, J.; Nagaveena, S.; Krishna Sharma, R.; Adam Khan, M.; More, C.V.; Rajini, N.; Varol, T. Development of Lightweight Polymer Laminates for Radiation Shielding and Electronics Applications. *Int. J. Polym. Sci.* **2022,** *2022*, 1–13.
(3) Verma, S.; Sanghi, S.; Amritphale, S. Development of Advanced, Non-Toxic, X-Ray Radiation Shielding Glass Possessing Barium, Boron Substituted Kornerupine Crystallites in the Glassy Matrix. *J. Inorg. Organomet. Polym. Mater.* **2018,** *28,* 35–49.
(4) Banerjee, S.; Bairagi, S.; Ali, S.W. A Critical Review on Lead-Free Hybrid Materials for Next Generation Piezoelectric Energy Harvesting and Conversion. *Ceram. Int.* **2021,** *47* (12), 16402–16421.
(5) Arif Sazali, M.; Alang Md Rashid, N.K.; Hamzah, K. A Review on Multilayer Radiation Shielding. In *IOP Conference Series: Materials Science and Engineering, 2019*; IOP Publishing, 2019; pp 1–8.
(6) Li, Q.; Wei, Q.; Zheng, W.; Zheng, Y.; Okosi, N.; Wang, Z.; Su, M. Enhanced Radiation Shielding with Conformal Light-Weight Nanoparticle–Polymer Composite. *ACS Appl. Mater. Interfaces* **2018,** *10* (41), 35510–35515.
(7) Bozkurt, M.; Şahin, N.; Karabul, Y.; Kılıç, M.; Özdemir, Z.G. Radiation Shielding Performances of Na_2SiO_3 Based Low-Cost Micro and Nano Composites for diagnostic imaging. *Prog. Nucl. Energy* **2022,** *143,* 104058.

(8) Langeveld, W.G. Effective Atomic Number, Mass Attenuation Coefficient Parameterization, and Implications for High-Energy X-Ray Cargo Inspection Systems. *Phys. Procedia* **2017**, *90*, 291–304.
(9) Нікіфоров, Ю.М.; Скоренький, Ю.Л. Fundamentals of Nuclear Physics. In 2012.
(10) Fornalski, K.W. Simple Empirical Correction Functions to Cross Sections of the Photoelectric Effect. Compton Scattering, Pair and Triplet Production for Carbon Radiation Shields for Intermediate and High Photon Energies. *J. Phys. Commun.* **2018**, *2* (3), 035038.
(11) Cheewasukhanont, W.; Limkitjaroenporn, P.; Sayyed, M.; Kothan, S.; Kim, H.; Kaewkhao, J. High Density of Tungsten Gadolinium Borate Glasses for Radiation Shielding Material: Effect of WO3 Concentration. *Radiat. Phys. Chem.* **2022**, *192*, 109926.
(12) Halimah, M.; Azuraida, A.; Ishak, M.; Hasnimulyati, L. Influence of Bismuth Oxide on Gamma Radiation Shielding Properties of Boro-Tellurite Glass. *J. Non-Cryst. Solids* **2019**, *512*, 140–147.
(13) Dole, L.R.; Quapp, W. Radiation Shielding Using Depleted Uranium Oxide in Nonmetallic Matrices. ORNL/TM-2002/111, Oak Ridge National Laboratory, UT-Battelle, LLC, Oak Ridge, Tennessee (August 2002) 2002.
(14) Bukhvalova, S.Y.; Asmolova, N.F.; Lopatina, T.I.; Bochkarev, M.N. Bismuth and thorium Fluorides as Efficient X-ray Radiation Shielding Materials. *Radiat. Phys. Chem.* **2021**, *182*, 109388.
(15) Gholamzadeh, L.; Sharghi, H.; Aminian, M.K. Synthesis of Barium-Doped PVC/Bi_2WO_6 Composites for X-Ray Radiation Shielding. *Nuclear Eng Technol* **2022**, *54* (1), 318–325.
(16) Chang, L.; Zhang, Y.; Liu, Y.; Fang, J.; Luan, W.; Yang, X.; Zhang, W. Preparation and Characterization of Tungsten/Epoxy Composites for γ-Rays Radiation Shielding. *Nucl. Instrum. Methods Phys. Res., Sect. B* **2015**, *356*, 88–93.
(17) Danthanavat, N.; Mongkolsuk, M.; Tochaikul, G.; Sriwongta, S.; Piyajaroenporn, A.; Lithreungnam, C.; Moonkum, N. Study of Epoxy Shielding Material with Barium Sulphate for Development of Radiation Protection Materials in Low-Dose Diagnostic X-ray. *Radiat. Eff. Defects Solids* **2021**, *176* (9–10), 887–895.
(18) Tochaikul, G.; Phattanasub, A.; Muanglay, C.; Thongcommak, W.; Majan, S.; Doungkrat, L.; Suntivattanatum, S.; Moonkum, N. Fabrication of Epoxy-Resin-Based Bismuth-Oxide Powder Radioactive Container for Technetium-99 m and Iodine-131 Radiopharmaceuticals. *Radiat. Eff. Defects Solids* **2023**, *187* (5–6), 620–633.
(19) Moonkum, N.; Pilapong, C.; Daowtak, K.; Tochaikul, G.J.P. Radiation Protection Device Composite of Epoxy Resin and Iodine Contrast Media for Low-Dose Radiation Protection in Diagnostic Radiology. *Polymer*. **2023**, *15* (2), 430.
(20) Ling, T.-C.; Poon, C.-S.; Lam, W.-S.; Chan, T.-P.; Fung, K.K.-L. X-Ray Radiation Shielding Properties of Cement Mortars Prepared with Different Types of Aggregates. *Mater. Struct.* **2013**, *46*, 1133–1141.
(21) Yao, Y.; Zhang, X.; Li, M.; Yang, R.; Jiang, T.; Lv, J. Investigation of Gamma Ray Shielding Efficiency and Mechanical Performances of Concrete Shields Containing Bismuth Oxide as an Environmentally Friendly Additive. *Radiat. Phys. Chem.* **2016**, *127*, 188–193.
(22) Kavaz, E.; Armoosh, S.; Perişanoğlu, U.; Ahmadi, N.; Oltulu, M. Gamma Ray Shielding Effectiveness of the Portland Cement Pastes Doped with Brass-Copper: An Experimental Study. *Radiat. Phys. Chem.* **2020**, *166*, 108526.
(23) Gharissah, M.S.; Ardiansyah, A.; Pauziah, S.R.; Muhammad, N.A.; Rahmat, R.; Heryanto, H.; Tahir, D. Composites Cement/$BaSO_4$/Fe_3O_4/CuO for Improving X-ray Absorption Characteristics and Structural Properties. *Sci. Rep.* **2022**, *12* (1), 19169.
(24) Sayyed, M.; Elsafi, M.; Almuqrin, A.H.; Cornish, K.; Elkhatib, A.M. Novel Shielding Mortars for Radiation Source Transportation and Storage. *Sustainability* **2022**, *14* (3), 1248.
(25) Sayyed, M.; Almousa, N.; Elsafi, M. Preparation of Mortar with Fe_2O_3 nanoparticles for radiation shielding application. *Coatings* **2022**, *12* (9), 1329.
(26) Aïtcin, P.-C. Portland Cement. In *Science and Technology of Concrete Admixtures*; Woodhead Publishing, 2016; pp 27–51.
(27) Widmark, J.M. Imaging-Related Medications: A Class Overview. *Proc. (Bayl. Univ. Med. Cent)*. **2007**, *20* (4), 408–417.
(28) Sanz, J.; Tomasa, O.; Jimenez-Franco, A.; Sidki-Rius, N. Barium (Ba)[Z = 56]. In *Elements and Mineral Resources*;Springer, 2022; pp 23–26.

(29) Oskarsson, A. Barium. In *Handbook on the Toxicology of Metals*; Academic Press, 2022; pp 91–100.
(30) Maghrabi, H.A.; Vijayan, A.; Deb, P.; Wang, L. Bismuth Oxide-Coated Fabrics for X-Ray Shielding. *Text. Res. J.* **2016,** *86* (6), 649–658.
(31) Sanz, J.; Tomasa, O.; Jimenez-Franco, A.; Sidki-Rius, N. Bismuth (Bi)[Z = 83]. In *Elements and Mineral Resources*; Springer, 2022; pp 31–33.
(32) El-Fiki, S.; El Kameesy, S.; Nashar, D.; Abou-Leila, M.; El-Mansy, M.; Ahmed, M. Influence of Bismuth Contents on Mechanical and Gamma Ray Attenuation Properties of Silicone Rubber Composite. *Int. J. Adv. Res* **2015,** *3* (6), 1035–1041.
(33) Scrivener, K.L. Options for the Future of Cement. *Indian Concr. J* **2014,** *88* (7), 11–21.
(34) Zhang, Y.; Napier-Munn, T. Effects of Particle Size Distribution, Surface Area and Chemical Composition on Portland Cement Strength. *Powder Technol.* **1995,** *83* (3), 245–252.
(35) Dubberke, W. *Factors Relating to Aggregate Durability in Portland Cement Concrete*. In Iowa. Dept. of Transportation. Highway Division: 1983.
(36) McLeod, R.S. Ordinary Portland Cement. *BFF Autumn* **2005,** *30,* 33.
(37) Singh, K.; Singh, H.; Sharma, V.; Nathuram, R.; Khanna, A.; Kumar, R.; Bhatti, S.S.; Sahota, H.S. Gamma-Ray Attenuation Coefficients in Bismuth Borate Glasses. *Nucl. Instrum. Methods Phys. Res., Sect. B* **2002,** *194* (1), 1–6.
(38) Singh, S.; Kumar, A.; Singh, D.; Thind, K.S.; Mudahar, G.S. Barium–Borate–Flyash Glasses: As Radiation Shielding Materials. *Nucl. Instrum. Methods Phys. Res., Sect. B* **2008,** *266* (1), 140–146.
(39) Xu, M.; Gong, S.; Niu, Y.; Zhang, K.; Liu, T.; Chen, Z. Bismuth-based Metal-Organic Frameworks Derived Rod-Like Nanoreactors for Neutral Aqueous Battery-Type Anode. *Science China Materials* **2023,** *66* (1), 106–117.
(40) Martin, C.J.; Sutton, D.G. *Practical Radiation Protection in Healthcare*; Oxford University Press, 2015.
(41) Protection, I.C.o.N.-I.R. ICNIRP Statement – Protection of Workers Against Ultraviolet Radiation. *Health Phys.* **2010,** *99* (1), 66–87.
(42) Chen, Z.; Cao, K.; Xia, Y.; Li, Y.; Hou, Y.; Wang, L.; Li, L.; Chang, L.; Li, W. Cellular Senescence in Ionizing Radiation. *Oncol. Rep.* **2019,** *42* (3), 883–894.
(43) Moonkum, N.; Wongpiem, U.; Sriwongta, S.; Danthanawat, N.; Tochaikul, G.; Pilapong, C. Effect of X-Ray Diagnostic Energy to Peripheral Blood Mononuclear Cells and CD34+/CD133+ Expression: An in vitro Study. *JCST* **2021,** *11* (1), 24–31.
(44) Tochaikul, G.; Danthanavat, N.; Pilapong, C.; Moonkum, N. Effect of Low Dose Radiation from General X-Ray to T-Cell Lymphocyte Expression Using an in vitro Method. *Radiat. Eff. Defects Solids* **2022,** *177*, 351–359.
(45) Tochaikul, G.; Pilapong, C.; Daowtak, K.; Moonkum, N. Influence of Radiation Dose from Repeated Chest X-Ray on Cell Morphology and Proliferation in Peripheral Blood Mononuclear Cells an in vitro Study. *Radiat. Eff. Defects Solids* **2023,** *178* (7–8), 929–937.
(46) O'Connor, M.J. Targeting the DNA Damage Response in Cancer. *Mol. Cell* **2015,** *60* (4), 547–560.
(47) Schulman, J.H.; Ginther, R.J.; Klick, C.C.; Alger, R.S.; Levy, R.A. Dosimetry of X-Rays and Gamma-Rays by Radiophotoluminescence. *J. Appl. Phys.* **1951,** *22* (12), 1479–1487.
(48) Fano, U. Penetration of Protons, Alpha Particles, and Mesons. *Annu. Rev. Nucl. Sci.* **1963,** *13* (1), 1–66.
(49) DellaGuardia, R.; Seeger, D.; Mauer IV, J. X-Ray Transmission Through Low Atomic Number Particles. *Microelectron. Eng.* **1989,** *9* (1–4), 139–142.
(50) Moonkum, N.; Pilapong, C.; Daowtak, K.; Tochaikul, G. Evaluation of Silicone Rubber Shielding Material Composites Enriched with $BaSO_4$ and Bi_2O_3 Particles for Radiation Shielding Properties. *Mater. Res. Innovations* **2023,** *27* (5), 296–303.
(51) Thumwong, A.; Chinnawet, M.; Intarasena, P.; Rattanapongs, C.; Tokonami, S.; Ishikawa, T.; Saenboonruang, K. A Comparative Study on X-ray Shielding and Mechanical Properties of Natural Rubber Latex Nanocomposites Containing Bi_2O_3 or $BaSO_4$: Experimental and Numerical Determination. *Polymers. (Basel)* **2022,** *14* (17), 3654.
(52) Abdolahzadeh, T.; Morshedian, J.; Ahmadi, S. Novel Polyethylene/Tungsten Oxide/Bismuth Trioxide/Barium Sulfate/Graphene Oxide Nanocomposites for Shielding Against X-Ray Radiations. *Int. J. Rad. Res.* **2023,** *21* (1), 79–87.

(53) Eckelt, A.; Eckelt, J.; Wolf, B. Solubility of Polymers. *Encyclopedia of Polymer Science and Technology* **2002,** *12*, 618–626.
(54) Bhogayata, A.C.; Arora, N.K. Impact Strength, Permeability and Chemical Resistance of Concrete Reinforced with Metalized Plastic Waste Fibers. *Constr. Build. Mater.* **2018,** *161,* 254–266.
(55) Rozenblat, Y.; Portnikov, D.; Levy, A.; Kalman, H.; Aman, S.; Tomas, J. Strength Distribution of Particles Under Compression. *Powder Technol.* **2011,** *208* (1), 215–224.
(56) Bhirud, Y.L.; Sangle, K.K.; Vaidya, O.V.; Patare, S.A. Influence of Higher Binder Content on the Splitting Tensile Strength and Modulus of Elasticity of Self-Compacting Concrete: An Experimental Investigation and Proposed Prediction Equation. *Constr. Build. Mater.* **2023,** *398,* 132478.
(57) Kilincarslan, S.; Akkurt, I.; Basyigit, C. The Effect of Barite Rate on Some Physical and Mechanical Properties of Concrete. *Mater. Sci. Eng. A* **2006,** *424* (1–2), 83–86.
(58) Restuccia, L.; Favero, A.; Jagdale, P.; Cavalot, G.; Ferro, G.A. Design of Bismuth Oxide Nanoparticles as Lightweight Aggregate in Cement Composites against X-Rays. *Mater. Des. Proc. Commun.* **2019,** *1* (2), e34.
(59) Abdolahzadeh, T.; Morshedian, J.; Ahmadi, S. Preparation and Characterization of Nano WO_3/Bi_2O_3/GO and $BaSO_4$/GO Dispersed HDPE Composites for X-Ray Shielding Application. *Polyolefins Journal* **2022,** *9* (2), 73–83.
(60) Nunez-Briones, A.; Benavides, R.; Bolaina-Lorenzo, E.; Martínez-Pardo, M.; Kotzian-Pereira-Benavides, C.; Mendoza-Mendoza, E.; Bentacourt-Galindo, R.; Garcia-Cerda, L. Nontoxic Flexible PVC Nanocomposites with Ta_2O_5 and Bi_2O_3 Nanoparticles for Shielding Diagnostic X-Rays. *Radiat. Phys. Chem.* **2023,** *202,* 110512.
(61) Malekzadeh, R.; Sadeghi Zali, V.; Jahanbakhsh, O.; Okutan, M.; Mesbahi, A. The Preparation and Characterization of Silicon-Based Composites Doped with $BaSO_4$, WO_3, and PbO Nanoparticles for Shielding Applications in PET and Nuclear Medicine Facilities. *Nanomed. J.* **2020,** *7* (4), 324–334.
(62) Abbas, M.I.; El-Khatib, A.M.; Elsafi, M.; El-Shimy, S.N.; Dib, M.F.; Abdellatif, H.M.; Baharoon, R.; Gouda, M.M. Investigation of Gamma-Ray Shielding Properties of Bismuth Oxide Nanoparticles with a Bentonite–Gypsum Matrix. *Materials. (Basel)* **2023,** *16* (5), 2056.
(63) Mirji, R.; Lobo, B. Radiation Shielding Materials: A Brief Review on Methods, Scope and Significance. In *Proceedings of the National Conference on 'Advances in VLSI and Microelectronics', 2017*; 2017; pp 96–100.
(64) Akkurt, İ.; Başyiğit, C.; Akkaş, A.; Kılınçarslan, Ş.; Mavi, B.; Günoğlu, K. Determination of Some Heavyweight Aggregate Half Value Layer Thickness Used for Radiation Shielding. *Acta Phys. Pol., A* **2012,** *121* (1), 138–140.
(65) AbuAlRoos, N.J.; Amin, N.A.B.; Zainon, R. Conventional and New Lead-Free Radiation Shielding Materials for Radiation Protection in Nuclear Medicine: A Review. *Radiat. Phys. Chem.* **2019,** *165,* 108439.
(66) Quapp, W.; Miller, W.; Taylor, J.; Hundley, C.; Levoy, N. DUCRETE^{TM}: A Cost Effective Radiation Shielding Material. *Spectrum* **2000,** *2000*, 24–28.
(67) Abdullah, M.A.H.; Rashid, R.S.M.; Amran, M.; Hejazii, F.; Azreen, N.; Fediuk, R.; Voo, Y.L.; Vatin, N.I.; Idris, M.I. Recent Trends in Advanced Radiation Shielding Concrete for Construction of Facilities: Materials and Properties. *Polymers. (Basel)* **2022,** *14* (14), 2830.
(68) Tyagi, G.; Singhal, A.; Routroy, S.; Bhunia, D.; Lahoti, M. Radiation Shielding Concrete with Alternate Constituents: An Approach to Address Multiple Hazards. *J. Hazard. Mater.* **2021,** *404,* 124201.
(69) Nawy, E.G. *Concrete Construction Engineering Handbook*; CRC Press, 2008.
(70) Naik, T.R., Sustainability of the Cement and Concrete Industries. In *Sustainable Construction Materials and Technologies*; CRC Press, 2020; pp 19–25.